

Constructing Priors that Penalize the Complexity of Gaussian Random Fields

Geir-Arne Fuglstad¹, Daniel Simpson², Finn Lindgren², and Håvard Rue¹

¹Department of Mathematical Sciences, NTNU, Norway

²Department of Mathematical Sciences, University of Bath, United Kingdom

June 19, 2022

Abstract

Gaussian random fields (GRFs) are important building blocks in hierarchical models for spatial data, but their parameters typically cannot be consistently estimated under in-fill asymptotics. Even for stationary Matérn GRFs, the posteriors for range and marginal variance do not contract and for non-stationary models there is a high risk of overfitting the data. Despite this, there has been no practically useful, principled approach for selecting the prior on their parameters, and the prior typically must be chosen in an *ad-hoc* manner. We propose to construct priors such that simpler models are preferred, i.e. shrinking stationary GRFs towards infinite range and no effect, and shrinking non-stationary extensions towards stationary GRFs.

We use the recent Penalised Complexity prior framework to construct a practically useful, tunable, weakly informative joint prior on the range and the marginal variance for a Matérn GRF with fixed smoothness. We then introduce extra flexibility in the covariance structure of the GRF through covariates and discuss how to extend the stationary prior. We apply the priors to a dataset of annual precipitation in southern Norway and show that the scheme for selecting the hyperparameters of the non-stationary extension leads to improved predictive performance over the stationary model.

Keywords: Bayesian, Penalised Complexity, Priors, Spatial models, Range, Non-stationary

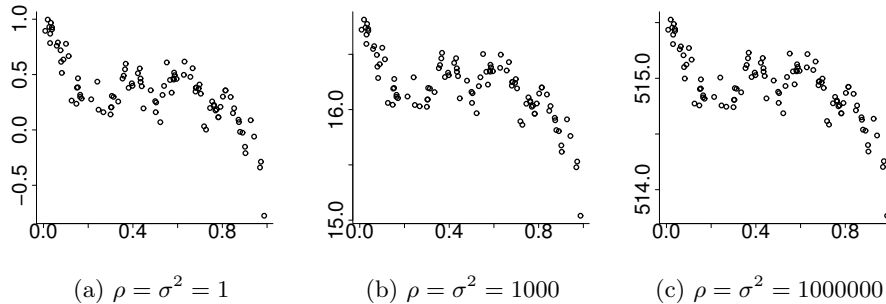


Figure 1: Simulations with the exponential covariance function $c(d) = \sigma^2 e^{-d/\rho}$ for different values of $\rho = \sigma^2$ using the same underlying realization of independent standard Gaussian random variables. The patterns of the values are almost the same, but the levels differ.

1 Introduction

Gaussian random fields (GRFs) provide a simple and powerful tool for introducing spatial or temporal dependence in a model and are fundamental building blocks in spatial statistics and non-parametric modelling, but even for stationary GRFs controlled only by range and marginal variance, the choice of prior distribution remains a challenge. The prior is difficult to choose: a well-chosen prior will stabilise the inference and improve the predictive performance, whereas a poorly chosen prior can be catastrophic. But since the parameters in the second-order structure of a GRF can affect the predictive distributions of the GRF in unexpected ways, it is difficult to construct good priors and the prior is typically chosen in an *ad-hoc* fashion.

We focus on the case where the stationary part of the GRF is a Matérn GRF with fixed smoothness, but the methods we develop are more widely applicable. The Matérn GRF has a ridge in the likelihood along which the value of the likelihood decreases slowly (Warnes and Ripley, 1987), and there is no consistent estimator under in-fill asymptotics for the range and the marginal variance (Stein, 1999; Zhang, 2004). The behaviour of the prior on the ridge will strongly affect the behaviour of the posterior on the ridge and no matter how many points are observed in a bounded observation window, there is a limit to the amount of information that can be learned about these parameters. For example, if a one-dimensional GRF with an exponential covariance function is observed on the interval $[0, 1]$, it is only the ratio of the range and the marginal variance that can be estimated consistently, and not the range and the marginal variance separately (Ying, 1991). When the range and marginal variance increase together, the marginal variance at each location changes, but conditional on the value at one location the remaining correlations between the locations change only slightly. Figure 1 shows how the level moves, but the pattern of the points around the level remains stable for increasing values of the range and the marginal variance.

Since there is a connection between what can be learned from data and what can affect the predictive distributions, the ratio of the range and the marginal variance is also the important quantity for the asymptotic predictions under in-fill when the exponential covariance function is used (Stein, 1999). But even though intrinsic models can be useful, a practitioner who observes the values in Figure 1a is unlikely to believe that the ranges and marginal variances that can generate Figures 1b and 1c are correct even if the spread is consistent with the observed pattern. Therefore, we believe the practitioner should be provided with a prior that allows him/her to include expert knowledge, in an interpretable way, about how far the posterior should be allowed to move along the ridge.

But to our knowledge, the only principled approach to prior selection for GRFs was introduced by Berger et al. (2001), who derived reference priors for a GRF partially observed with no noise. These priors fundamentally depend on the design of the experiment, which makes them inappropriate as “blind” default priors or when data is being analysed in a sequential fashion, and they have no option to include expert knowledge about the typical size of the spatial effect and are thus not appropriate for achieving credible intervals that are consistent with prior knowledge.

The work on reference priors have been extended by several authors (Paulo, 2005; Kazianka and Pilz, 2012; Kazianka, 2013) – critically Oliveira (2007) allowed for Gaussian observation noise – however, these papers have the same design dependency as the original work. Perhaps most importantly, the priors are not applicable for many hierarchical models because the assumption of Gaussian observation noise and linear covariates is insufficient in many applications and there are currently no extensions of spatial reference priors to other observation processes. In the more restricted case of a GRF with a Gaussian covariance function van der Vaart and van Zanten (2009) showed that the inference asymptotically behaves well with an inverse gamma distribution on range, but they provide no guidance on which hyperparameters should be selected for the prior.

In practice, the range is commonly given a uniform distribution on a bounded interval, a log-uniform distribution on a bounded interval or an inverse gamma distribution with infinite variance and the mean placed at an appropriate location. These priors have little theoretical foundation and are *ad-hoc* choices based on the idea that they will allow reasonable ranges, but Berger et al. (2001) noted that the posterior inference can be sensitive to the choice of cut-off for the uniform prior, and it is necessary with careful sensitivity analysis. The bounded intervals are necessary because improper prior distributions cannot be applied for the parameters of a GRF without great care as they tend to lead to improper posterior distributions. From a Bayesian modelling perspective this is an unsatisfactory situation because the prior is supposed to encode the user’s prior knowledge and uncertainty about the parameters, and not be an *ad-hoc* choice made out of convenience without theoretical justification.

We propose to use the recent Penalised Complexity (PC) prior framework developed by Simpson et al. (2015) to construct a new, principled joint prior for the range and the marginal variance of a Matérn GRF. The PC prior framework ignores the observation process entirely and focuses instead on the geometry of the parameter space induced by the infinite-dimensional GRF. This is more technically demanding than considering finite-

dimensional observations, like for the reference priors, but we are able to use the resulting prior for any spatial design and any observation process. The second key difference between the reference priors and the PC prior approach is that while the former is non-informative in a technical sense, PC priors are weakly informative and, therefore, include specific information from the user. In particular, PC priors need a point in the parameter space, considered a *base model*, and hyperparameters that indicates how strongly the user wishes to shrink towards the base model. Simpson et al. (2015) showed that the resulting inference was quite robust against the specification of the hyperparameters.

This provides a way to limit how far the stationary GRF can move towards near-intrinsic models on the ridge, but usually one tends to believe that there also should be some degree of non-stationarity in the covariance structure of the GRF. However, adding this extra flexibility can lead to overfitting and one must be careful in selecting the prior on the extra flexibility. Since the covariance structure of a GRF is only observed indirectly through the values of the process and since there is no information about the covariances for locations without observations, the estimated covariance structure can be highly influenced by the types of non-stationarities allowed and the prior used. We extend the PC prior developed for the stationary Matérn GRF to a prior for a non-stationary GRF where the non-stationarity is controlled by covariates. The prior is motivated by g -priors and shrinkage properties, and we consider one scheme for selecting the hyperparameters that reduces the risk of overfitting the non-stationary GRF.

We start by deriving the new, joint PC prior for the range and the marginal variance of a Matérn GRF with fixed smoothness parameter in Section 2. Then in Section 3 the frequentist coverage is studied through a simulation study and compared with the coverage obtained using the Jeffreys' rule prior and *ad-hoc* uniform and log-uniform priors. In Section 4 we study the behaviour of the joint posterior under the PC-prior and the Jeffreys' rule prior and discuss the difference in behaviour. Then the frequentist properties of spatial logistic regression are studied in Section 5 to demonstrate the applicability of the PC prior for a non-Gaussian observation process. In Section 6 we discuss how to extend the prior for the stationary model to a prior for a non-stationary GRF and consider an application to annual precipitation in southern Norway. The paper ends with discussion and concluding remarks in Section 7.

2 Penalised complexity prior for the Matérn GRF

2.1 Background

The principle idea of the PC-prior framework is to think of each model component as a flexible extension of a simpler, less flexible *base model*. For example, a random effect with non-zero variance is considered an extension of a random effect with zero variance, i.e. no random effect. After choosing the base model for the component, one derives a distance measure from the base model to the models described by other parameter values. This distance quantifies how much more flexible the model is for other parameter values than the base model, and provides a measure of complexity for the model component. The

prior is then set directly on the distance from the base model instead of on the parameters of the model. This provides an improved way of setting priors on parameters for which it is hard to have intuition. For example, correlation parameters close the border values -1 , 0 and 1 , or the range in spatial models.

We measure the extra complexity of each model compared to the base model through the Kullback-Leibler divergence (KLD). The KLD of the probability density f from the probability density g is defined by

$$D_{\text{KL}}(f||g) = \int_{\mathcal{X}} f(\mathbf{x}) \log \left(\frac{f(\mathbf{x})}{g(\mathbf{x})} \right) d\mathbf{x},$$

and expresses the information lost when g is used to approximate f . The asymmetry of the KLD fits well with the asymmetric idea of preferring the base model, and we turn the KLD into a uni-directional distance from the base model g to the model f through $d(f||g) = \sqrt{2\text{KLD}(f||g)}$.

Simpson et al. (2015) provide three principles for setting the prior on the distance: Occam's razor, constant rate penalisation and user-defined scaling. Occam's razor is achieved by constructing a prior that penalises deviations from the base model and favours the base model until the data provides evidence against it. This suggests that the prior density should have its peak at distance 0 and decrease with increasing distance. The constant rate penalisation is achieved by making the prior on the distance, d , satisfy the relationship

$$\frac{\pi(d + \delta)}{\pi(d)} = r^\delta, \quad d, \delta \geq 0,$$

for a constant decay-rate $0 < r < 1$. For this choice, the relative change in the prior when the distance increases by δ does not depend on the current distance d , and the result is the exponential distribution $\pi(d) = \lambda \exp(-\lambda d)$.

The hyperparameter λ is set based on the final principle of user-defined scaling. We transform the distance back to an interpretable size $Q(d)$ and include prior information through, for example, $\text{P}(Q(d) > U) = \alpha$ or $\text{P}(Q(d) < L) = \alpha$, where U or L is an upper or lower limit, respectively, and α is the probability in the upper or lower tail of the prior distribution. By selecting U or L , and α the user combines prior belief with a prior derived from the geometry of the parameter space.

We want to extend the approach outlined above to Gaussian Matérn fields with fixed smoothnesses. We consider GRFs with the covariance function

$$C(d) = \sigma^2 \frac{1}{\Gamma(\nu)2^{\nu-1}} \left(\frac{\sqrt{8\nu d}}{\rho} \right)^\nu K_\nu \left(\frac{\sqrt{8\nu d}}{\rho} \right),$$

where the spatial range ρ and the marginal variance σ^2 must be estimated, and the smoothness ν is considered fixed. However, in general, the KLD between two arbitrary choices of parameters (ρ_0, σ_0^2) and (ρ_1, σ_1^2) is infinite when the GRF is observed at all locations in a bounded observation window. And to facilitate the construction of the prior, we select a parametrization of the spatial field that more accurately describes what can be and what cannot be consistently estimated under in-fill asymptotics.

We introduce the parameters $\kappa = \sqrt{8\nu}/\rho$ and

$$\tau = \frac{\Gamma(\nu)}{(4\pi)^{d/2}\Gamma(\nu + d/2)\sigma^2\kappa^{2\nu}},$$

which are a slight re-parametrization of the SPDE in Lindgren et al. (2011),

$$(\kappa^2 - \Delta)^{\alpha/2}(\sqrt{\tau}u(\mathbf{s})) = \mathcal{W}(\mathbf{s}), \quad \mathbf{s} \in \mathbb{R}^d, \quad (1)$$

where $\Delta = \frac{\partial^2}{\partial x^2} + \frac{\partial^2}{\partial y^2}$ is the Laplacian and \mathcal{W} is standard Gaussian white noise. If κ and τ are chosen as above, the SPDE specifies a Matérn GRF with range ρ , marginal variance σ^2 and smoothness $\nu = \alpha - d/2$.

In this parametrization τ can be consistently estimated under in-fill asymptotics, whereas κ cannot. If κ is kept fixed and the value of τ changes, the KLD is infinite, but if the value of τ is kept fixed and the value of κ changes, the KLD is finite. We use a two-step procedure for constructing the joint prior where we first set a prior for κ through the KLD of the GRF and then set a prior on τ given the value of κ through a consideration of finite-dimensional observations. When constructing the prior for κ , we use the base model $\kappa = 0$, which corresponds to an intrinsic GRF similar to a spline model, and when constructing the prior for $\tau|\kappa$, we use the base model $\tau = \infty$ for the fixed value of κ . This leads to a combination of shrinkage towards infinite range and zero marginal variance.

2.2 Joint prior for range and marginal variance

We fix τ and calculate the distance function for κ using the intrinsic base model $\kappa = 0$. The technical derivation is given in Appendix A and results in a distance function

$$d(\kappa) \propto \kappa^{d/2} \quad (2)$$

that provides a quantification of how far the distribution of the GRF is from the intrinsic GRF as a function of κ . Since $\rho = \sqrt{8\nu}/\kappa$, Equation (2) implies that the distance behaves as $\rho^{-d/2}$ if the marginal variance increases in such a way that τ is kept constant.

The proportionality constant in the distance expression is not important and we set it to 1 and set an exponential prior on the distance, which leads to a prior on κ given by

$$\pi(\kappa) = \lambda_1 \exp(-\lambda_1 d(\kappa)) \left| \frac{d}{d\kappa} d(\kappa) \right| = \frac{\lambda_1 d}{2} \kappa^{d/2-1} \exp(-\lambda_1 \kappa^{d/2}), \quad \kappa > 0, \quad (3)$$

where λ_1 can be selected by controlling the *a priori* probability that the range is below a specific limit, $P(\sqrt{8\nu}/\kappa < \rho_0) = \alpha_1$. After selecting the lower range, ρ_0 , and the probability in the lower tail, α_1 , the expression $\lambda_1 = -\log(\alpha_1)(\rho_0/\sqrt{8\nu})^{d/2}$ can be used to calculate the associated hyperparameter.

If the process were observed at all locations on a bounded observation window, the value of τ would be exactly determined. A prior for τ is needed because in practice we only observe a finite-dimensional part of the GRF. We make the assumption that we

are interested in observing finite-dimensional quantities that arise by applying a linear operator on the spatial field, i.e. $\pi(\mathbf{u}|\kappa, \tau) \propto \exp(-\tau \mathbf{u}^T \Sigma^{-1} \mathbf{u}/2)$. The covariance matrix Σ only depends on κ and not τ , and the parameter τ acts as the precision parameter. We use the PC prior for the precision parameter in a multivariate Gaussian constructed by Simpson et al. (2015) (with base model $\tau = \infty$),

$$\pi_{\text{PC}}(\tau) = \frac{\lambda_2}{2} \tau^{-3/2} \exp(-\lambda_2 \tau^{-1/2}), \quad \tau > 0, \quad (4)$$

where we can set λ_2 by controlling the *a priori* probability that the marginal variance exceeds a specific level,

$$\text{P} \left(\sigma^2 = \frac{C(\nu)}{\tau \kappa^{2\nu}} > \sigma_0^2 \middle| \kappa \right) = \alpha_2. \quad (5)$$

The constant

$$C(\nu) = \frac{\Gamma(\nu)}{\Gamma(\nu + d/2)(4\pi)^{d/2}}$$

is the constant needed to make the left-hand side of the inequality equal to the marginal variance of the GRF.

Since the criterion in Equation (5) is conditional on the value of κ , it introduces dependence between κ and τ in the joint prior. We write Equation (5) as

$$\text{P} \left(\tau < \frac{C(\nu)}{\kappa^{2\nu} \sigma_0^2} \middle| \kappa \right) = \alpha_2$$

and find

$$\begin{aligned} \exp \left(-\lambda_2 \left(\frac{C(\nu)}{\kappa^{2\nu} \sigma_0^2} \right)^{-1/2} \right) &= \alpha_2, \\ \lambda_2 &= \frac{\lambda_3}{\kappa^\nu}, \end{aligned}$$

where λ_3 absorbs the other constants in λ_2 . We insert this into Equation (4) and find the conditional distribution

$$\pi(\tau|\kappa) = \frac{\lambda_3 \tau^{-3/2}}{2\kappa^\nu} \exp(-\lambda_3 \kappa^{-\nu} \tau^{-1/2}). \quad (6)$$

This implies that the dependence between κ and τ is affected by the value of the smoothness ν .

The joint prior on κ and τ is found by combining Equation (3) and Equation (6), and is given by

$$\pi(\kappa, \tau) = \pi(\kappa) \pi(\tau|\kappa) = \frac{\lambda_1 \lambda_3 d}{4} \tau^{-3/2} \kappa^{d/2-1-\nu} \exp(-\lambda_1 \kappa^{d/2} - \lambda_3 \kappa^{-\nu} \tau^{-1/2}).$$

There is a one-to-one correspondence between κ and τ , and ρ and σ^2 ,

$$\begin{bmatrix} \rho \\ \sigma^2 \end{bmatrix} = \begin{bmatrix} \sqrt{8\nu} \\ \frac{C(\nu)}{\kappa^{2\nu} \tau} \end{bmatrix},$$

which can be exploited to transform the joint prior for κ and τ to the joint prior for ρ and σ^2 .

Main result 2.1. *Joint prior for the range and marginal variance of a Matérn GRF*

$$\pi(\rho, \sigma^2) = \left[\frac{d\lambda_4}{2} \rho^{-1-d/2} \exp\left(-\lambda_4 \rho^{-d/2}\right) \right] \left[\frac{\lambda_5}{2} \sigma^{-1} \exp(-\lambda_5 \sigma) \right], \quad (7)$$

where λ_4 and λ_5 are selected according to the a priori statements

$$P(\rho < \rho_0) = \alpha_4 \quad \text{and} \quad P(\sigma^2 > \sigma_0^2) = \alpha_5,$$

which give $\lambda_4 = -\rho_0^{d/2} \log(\alpha_4)$ and $\lambda_5 = -\frac{\log(\alpha_5)}{\sigma_0}$.

3 Frequentist coverage

The series of papers on reference priors for GRFs starting with Berger et al. (2001) evaluated the priors by studying frequentist properties of the resulting Bayesian inference. If a prior is intended as a default prior, it should lead to good frequentist properties such as a frequentist coverage of the equal-tailed $100(1 - \alpha)\%$ Bayesian credible intervals that is close to the nominal $100(1 - \alpha)\%$. The PC prior is not an objective prior and it is not intended to be non-informative, but the sensitivity of the posterior to the prior specification is important. We follow their design with one key difference: we do not include covariates and measurement noise. The reference priors are not proper distributions and the goal of the series of papers was to derive them for different situations such as a spatial field combined with covariates, and a spatial field combined with covariates and Gaussian measurement noise. However, in this paper we are constructing a prior for the GRF component itself and we are *not* constructing a prior for the GRF together with covariates or together with covariates and Gaussian measurement noise. This is possible because the PC-prior is a proper distribution and can be applied to a spatial field together with covariates and arbitrary observation processes without breaking the properness of the posterior.

The study uses an isotropic GRF, u , with an exponential covariance function $c(d) = \exp(-2d/\rho_0)$ observed at the locations shown in Figure 2. The observation locations were randomly selected within the domain $[0, 1]^2$ and are distributed in an irregular pattern. The study is performed for two values of the nominal range: a short range, $\rho_0 = 0.1$, and a long range, $\rho_0 = 1$. We generate multiple realizations and for each realization we assume that the field is observed directly and fit the model

$$y_i = u(\mathbf{s}_i), \quad i = 1, 2, \dots, 25,$$

where u is a GRF with an exponential covariance function with unknown parameters ρ and σ^2 . We apply four different priors: the PC-prior (PriorPC), the Jeffreys' rule prior (PriorJe), a uniform prior on range on a bounded interval combined with the Jeffreys' prior for variance (PriorUn1) and a uniform prior on the log-range on a bounded interval

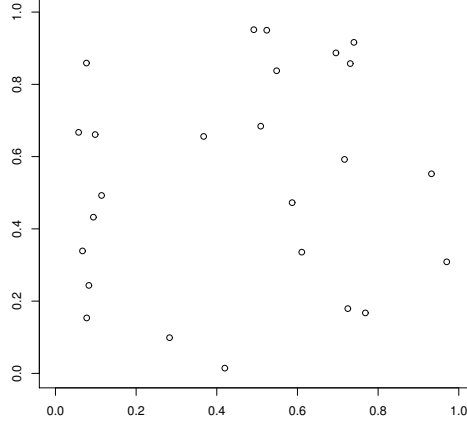


Figure 2: Spatial design for the simulation study of frequentist coverage.

Table 1: The four different priors used in the study of frequentist coverage. The Jeffreys' rule prior uses the spatial design of the problem through $U = (\frac{\partial}{\partial \rho} \Sigma) \Sigma^{-1}$, where Σ is the correlation matrix of the observations (See Berger et al. (2001)).

Prior	Expression	Parameters
PriorPC	$\pi_1(\rho, \sigma) = \lambda_1 \lambda_2 \rho^{-2} \exp(-\lambda_1 \rho^{-1} - \lambda_2 \sigma)$	$\rho, \sigma > 0$ Hyperparameters: $\alpha_\rho, \rho_0, \alpha_\sigma, \sigma_0$
PriorJe	$\pi_2(\rho, \sigma) = \sigma^{-1} \left(\text{tr}(U^2) - \frac{1}{n} \text{tr}(U)^2 \right)^{1/2}$	$\rho, \sigma > 0$ Hyperparameters: None
PriorUn1	$\pi_3(\rho, \sigma) \propto \sigma^{-1}$	$\rho \in [A, B], \sigma > 0$ Hyperparameters: A, B
PriorUn2	$\pi_4(\rho, \sigma) \propto \sigma^{-1} \cdot \rho^{-1}$	$\rho \in [A, B], \sigma > 0$ Hyperparameters: A, B

combined with the Jeffreys' prior for variance (PriorUn2). The full expressions for the priors are given in Table 1.

For each choice of prior and hyperparameters we generate 1000 observation vectors $\mathbf{y} = (y_1, y_2, \dots, y_{25})$ and estimate the equal-tailed 95% credible intervals for range and marginal variance for each observation by running an MCMC-chain. The number of times the true value is contained within the estimated credible interval is divided by 1000 and given as the estimate of the frequentist coverage. PriorJe has no hyperparameters, but PriorPC, PriorUn1 and PriorUn2 each has hyperparameters that need to be set before using the prior. For PriorUn1 and PriorUn2 it is hard to give guidelines about which values should be selected since the main purpose of limiting the prior distributions to a bounded interval is to avoid an improper posterior and the choice tends to be *ad-hoc*. For PriorPC, on the other hand, there is a interpretable expression to choose the hyperparameters, which helps give an idea about which prior assumptions the chosen hyperparameters are expressing.

For PriorPC we need to make an *a priori* decision about the scales of the range and the marginal variance. The prior is set through four hyperparameters that describe our prior beliefs about the spatial field. We use

$$P(\rho < \rho_0) = 0.05$$

for $\rho_0 = 0.025\rho_T$, $\rho_0 = 0.1\rho_T$, $\rho_0 = 0.4\rho_T$ and $\rho_0 = 1.6\rho_T$, where ρ_T is the true range. This covers a prior where ρ_0 is much smaller than the true range, two priors where ρ_0 is smaller than the true range, but not far away, and one prior where ρ_0 is higher than the true range. For the marginal variance we use

$$P(\sigma^2 > \sigma_0^2) = 0.05,$$

for $\sigma_0 = 0.625$, $\sigma_0 = 2.5$, $\sigma_0 = 10$ and $\sigma_0 = 40$. We follow the same logic as for range and cover too small and too large σ_0 and two reasonable values. For PriorUn1 and PriorUn2, we set the lower and upper limits for the nominal range according to the values $A = 0.05$, $A = 0.005$ and $A = 0.0005$, and $B = 2$, $B = 20$ and $B = 200$. Some of the values are intentionally extreme to see the effect of misspecification.

The results for PriorPC are given in Tables 2 and 3 for the true ranges $\rho_T = 0.1$ and $\rho_T = 1$, respectively, and the tables for PriorUn1 and PriorUn2 are given in Appendix B. PriorJe resulted in 97.0% coverage with average length of the credible intervals of 0.86 for range and 96.0% coverage and average length of the credible intervals of 2.7 for marginal variance for $\rho_0 = 0.1$, and 95.4% coverage with average length of the credible intervals of 445 for range and 94.4% coverage with average length of the credible intervals of 355 for variance for $\rho_0 = 1$. The results show that for PriorPC, PriorUn1 and PriorUn2 the coverage and the length of the credible intervals are dependent on the choice of hyperparameters. This is not surprising since there are few observation and there is a ridge in the likelihood where the posterior behaviour is strongly dependent on the the prior. The lengths of the credible intervals are, in general, more well-behaved for $\rho_0 = 0.1$ than for $\rho_0 = 1$ because there is more information about the range available in the domain when the range is shorter.

Table 2: Frequentist coverage of 95% credible intervals for range and marginal variance when the range $\rho_0 = 0.1$ using PriorPC, where the average lengths of the credible intervals are shown in brackets.

(a) Range				
$\rho_0 \backslash \sigma_0$	40	10	2.5	0.625
0.025	0.768 [0.25]	0.749 [0.24]	0.760 [0.20]	0.693 [0.17]
0.1	0.965 [0.35]	0.976 [0.29]	0.961 [0.27]	0.937 [0.21]
0.4	0.990 [0.45]	0.989 [0.41]	0.993 [0.33]	0.987 [0.25]
1.6	0.717 [0.98]	0.692 [0.82]	0.756 [0.54]	0.807 [0.34]

(b) Marginal variance				
$\rho_0 \backslash \sigma_0$	40	10	2.5	0.625
0.025	0.941 [1.5]	0.952 [1.4]	0.957 [1.3]	0.918 [0.97]
0.1	0.953 [1.6]	0.966 [1.5]	0.944 [1.4]	0.927 [0.98]
0.4	0.953 [2.0]	0.952 [1.8]	0.960 [1.5]	0.943 [1.1]
1.6	0.904 [3.9]	0.906 [3.2]	0.939 [2.2]	0.972 [1.3]

Table 3: Frequentist coverage of 95% credible intervals for range and marginal variance when the true range $\rho_0 = 1$ using PriorPC, where the average lengths of the credible intervals are shown in brackets.

(a) Range				
$\rho_0 \backslash \sigma_0$	40	10	2.5	0.625
0.025	0.950 [12]	0.945 [7.1]	0.906 [3.2]	0.821 [1.4]
0.1	0.977 [15]	0.966 [8.2]	0.962 [3.6]	0.866 [1.5]
0.4	0.965 [26]	0.981 [13]	0.992 [5.1]	0.988 [1.8]
1.6	0.159 [74]	0.349 [31]	0.700 [11]	0.954 [3.3]

(b) Marginal variance				
$\rho_0 \backslash \sigma_0$	40	10	2.5	0.625
0.025	0.944 [11]	0.956 [6.2]	0.933 [2.8]	0.797 [1.1]
0.1	0.957 [13]	0.966 [7.2]	0.954 [3.1]	0.865 [1.2]
0.4	0.943 [23]	0.957 [11]	0.987 [4.4]	0.972 [1.5]
1.6	0.441 [68]	0.534 [29]	0.797 [9.1]	0.984 [2.5]

For PriorUn1 the coverage and the length of the credible intervals are strongly dependent on the upper limit in the prior. The prior has the undesirable property of including stronger and stronger prior belief in high ranges when the upper limit is increased. In practice the upper limit is unlikely to be chosen as extreme as in the example, but it verifies the observation of Berger et al. (2001) that the inference is sensitive to the hyperparameters for this prior. For PriorUn2 the coverage is good in both the short range and long range case, but the lengths of the credible intervals are sensitive to the upper limit of the prior.

The results show that the coverage for PriorPC is stable when a too low lower limit for range or a too high upper limit for variance is specified, but that specifying a too high lower limit for the range or a too low upper limit for variance produces large changes in the coverage. This is not unreasonable as the prior is then explicitly stating that the true value for range or variance is unlikely. The average length of the credible intervals are more sensitive to the hyperparameters than the coverages, but we see less extreme sizes for the credible intervals than for PriorJe.

The coverage of PriorJe is good, but the credible intervals seem excessively long and the prior is more computationally expensive than the other priors. PriorJe is only computationally feasible for low numbers of points since there is a cubic increase in the complexity as a function of the number of observations. The average length of the credible intervals for $\rho_0 = 1$ for marginal variance is 355, which imply unreasonably high standard deviations. The high standard deviations do not seem consistent with an observation with values contained between -3 and 3 . We study the credible intervals for PriorPC and PriorJe closer for a specific realization in the next section to gain intuition about why this happen.

With respect to computation time and ease of use versus coverage and length of credible intervals PriorUn2 and PriorPC appear to be the best choices. If coverage is the only concern, PriorUn2 performs the best, but if one also wants to control the length of the credible intervals by disallowing unreasonably high variances, PriorPC offers the most interpretable alternative. In a realistic situation it is probable that the researcher has prior knowledge, for example, that the spatial effect should not be greater than, say 4, and by encoding this information in PriorPC we can limit the upper limits of the credible intervals both for range and marginal variance.

4 Behaviour of the joint posterior

The extreme length of the credible intervals seen for the Jeffreys' rule prior are not entirely surprising due to the ridge in the likelihood, but they are troubling for interpreting the parameters. In the previous section we only looked at properties of the marginal credible intervals, but these do not tell the entire story because there is strong dependence between range and marginal variance in the joint posterior distribution. We study this dependence by studying the posterior distribution for the realization shown in Figure 3. The true range used to simulate the realization is 1. We use an MCMC sampler to draw samples from the joint posterior using the PC-prior with parameters $\alpha_\rho = 0.05$, $\rho_0 = 0.1$,

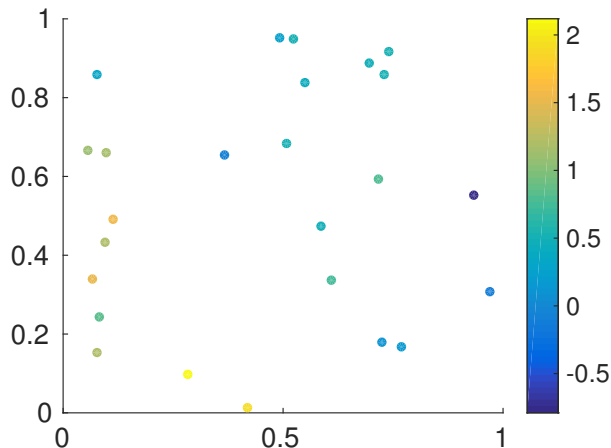


Figure 3: One realization of a GRF with the covariance function $c(d) = \exp(-2d)$ at 25 selected locations.

$\alpha_\sigma = 0.05$ and $\sigma_0 = 10$, and we draw samples from the joint posterior using the Jeffreys' rule prior.

Figure 4 shows that the upper tails of the posteriors when using the Jeffreys' rule prior are heavier than the upper tails of the posteriors when using the PC-prior. The lower endpoints of the credible intervals are similar for both priors, but there is a large difference in the upper limits because the likelihood decays slowly along the ridge. The marginal posterior distributions do not show the full story about the inference on range and marginal variance because the two parameters are strongly dependent in the posterior distribution. The PC-prior for the range has a heavy upper tail and the upper tail of the posterior for the range is controlled through the prior on the marginal variances. The large difference in the marginal posteriors for the nominal range in Figure 4a can be explained by the behaviour of the joint posterior.

Figure 5 shows the strong posterior dependence between nominal range and standard deviation in the tail of the distribution. Stein (1999) showed that the ratio of range and marginal variance is the important quantity for asymptotic predictions with the exponential covariance function. So the long tails are not a major concern for predictions, but they pose a concern for the interpretability of range and marginal variance. The values of all the observations in Figure 3 lie within the range -1 to 3 and it is unlikely that the true standard deviation should be on the order of 20 . Intrinsic models have a place in statistics, but the results show that the Jeffreys' rule prior has the, potentially, undesirable behaviour of favouring intrinsic GRFs with large marginal standard deviations and ranges even though they might not be physically reasonable. The PC prior offers a way to introduce prior belief about the size of the marginal standard deviations, and thus a way to reduce the preference for the intrinsic GRFs.

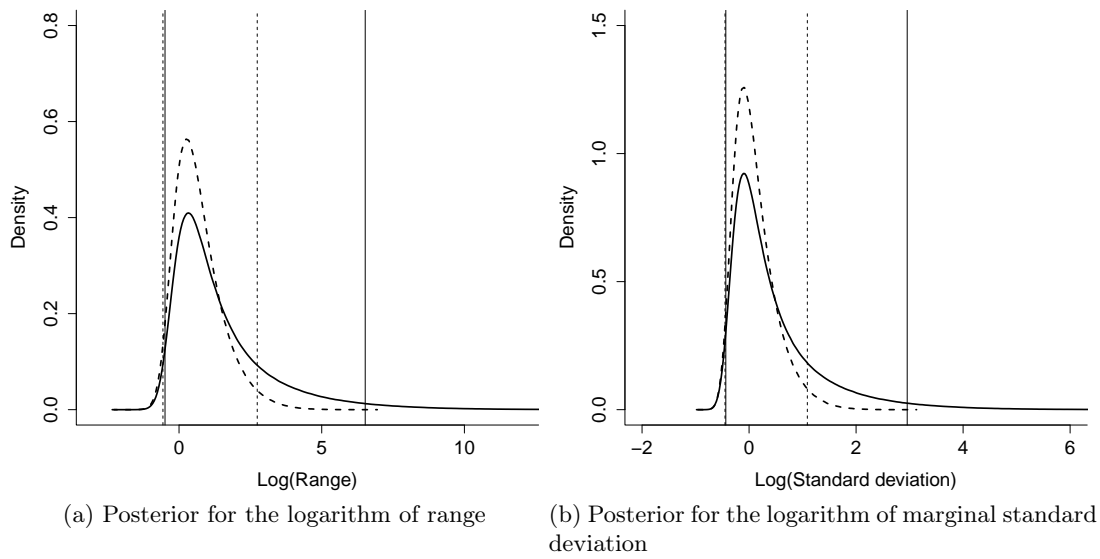


Figure 4: Marginal posteriors of the logarithm of range and the logarithm of marginal standard deviation. The dashed lines shows the posterior and the credible intervals when the PC-prior is used and the solid line shows the posterior and the credible intervals when the Jeffreys' rule prior is used.

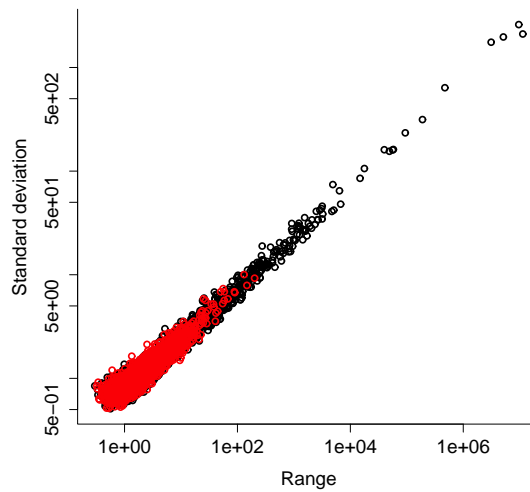


Figure 5: Samples from the joint posterior of range and marginal standard deviation. The red circles are samples using the PC-prior and the black circles are samples using the Jeffreys' rule prior.

5 Example: Spatial logistic regression

What makes the PC prior more practically useful than the reference prior, beyond the computational benefits and the interpretability, is that the prior is applicable in any hierarchical model and does not have to be re-derived each time a component is removed or added, or the observation process is changed. We consider a simple spatial logistic regression example to demonstrate the applicability of the PC prior beyond direct observations or Gaussian measurement noise.

We select the 25 locations in Figure 2 and generate realizations from the model

$$y_i | p_i \sim \text{Binomial}(20, p_i), \quad i = 1, 2, \dots, 25,$$

where

$$\text{probit}(p_i) = u(\mathbf{s}_i),$$

where u is a GRF with the exponential covariance function with parameters $\rho = 0.1$ and $\sigma = 1$. For each realization the parameters ρ and σ^2 are assumed unknown and must be estimated. The posteriors of the parameters are estimated with an MCMC chain and the equal-tailed 95% credible intervals are estimated from the samples of the MCMC-chain after burn-in. We repeat the procedure above 500 times and report the number of times the true value is contained in the credible interval and the average length of the credible interval.

The experiment is repeated for 64 different settings of the prior: the hyperparameter ρ_0 varies over $\rho_0 = 0.0025, 0.01, 0.04, 0.16$ and the hyperparameter σ_0 varies over $\sigma_0 = 40, 10, 2.5, 0.625$. This covers a broad range of values from too small to too large. The values in Table 4 are similar to the values in Table 2 except that the credible intervals are slightly longer. The longer credible intervals are reasonable since the binomial likelihood gives less information about the spatial field than direct observation of the spatial field. The coverage for marginal variance is good even for grossly miscalibrated priors, but the coverage for range is sensitive to bad calibration for range and the coverage is somewhat higher than nominal for the well-calibrated priors. This is a feature also seen in the directly observed case in Section 3.

6 Prior for extra flexibility in the covariance structure

Neither stationary nor non-stationary GRFs provide true representations of reality, but the extra flexibility in the covariance structure of a non-stationary GRF may provide a better fit to the data than the less flexible covariance structure of a stationary GRF. We will not be working under the stationary/non-stationary dichotomy, but instead under the more pragmatic viewpoint that all datasets are non-stationary to some degree. As long as the parametrization of the non-stationary GRF contains the stationary GRF as a special case, the added flexibility should improve the predictions if the prior is conservative enough to prevent the model from overfitting.

Ingebrigtsen et al. (2014) expanded the parameters of the SPDE in Equation (1) into spatially varying functions, $\log(\kappa(\cdot))$ and $\log(\tau(\cdot))$, through low-dimensional bases

Table 4: Frequentist coverage of the 95% credible intervals for range and marginal variance when the true range is 0.1 and true marginal variance is 1, where the average length of the credible intervals are given in brackets, for the spatial logistic regression example.

(a) Range				
$\rho_0 \backslash \sigma_0$	40	10	2.5	0.625
0.025	0.804 [0.29]	0.790 [0.24]	0.774 [0.22]	0.726 [0.19]
0.1	0.974 [0.41]	0.986 [0.37]	0.974 [0.33]	0.956 [0.24]
0.4	0.996 [0.61]	0.982 [0.57]	0.996 [0.43]	0.992 [0.30]
1.6	0.648 [1.4]	0.604 [1.2]	0.722 [0.67]	0.762 [0.44]

(b) Marginal variance				
$\rho_0 \backslash \sigma_0$	40	10	2.5	0.625
0.025	0.942 [2.0]	0.946 [1.9]	0.948 [1.7]	0.912 [1.2]
0.1	0.920 [2.3]	0.942 [2.0]	0.964 [1.8]	0.922 [1.2]
0.4	0.952 [2.7]	0.962 [2.4]	0.968 [1.9]	0.928 [1.2]
1.6	0.904 [5.3]	0.936 [4.1]	0.966 [2.7]	0.982 [1.5]

using a small number of covariates, and used independent Gaussian priors for the extra parameters. However, they experienced numerical problems and prior sensitivity, and Ingebrigtsen et al. (2015) developed an improved scheme for selecting the hyperparameters of the priors based on the properties of the resulting spatially varying local ranges and marginal variances. However, the inherent problem of their specification is that $\kappa(\cdot)$ affects both the correlation structure and the marginal variances of the spatial field. This makes it challenging to set priors on $\kappa(\cdot)$ and $\tau(\cdot)$, and we aim to improve their procedure by first improving the parametrization of the non-stationarity, and then developing a prior using the improved parametrization.

6.1 Parametrizing the extra flexibility

Instead of adding spatial variation to the coefficients of the SPDE in Equation (1), κ and τ , one can vary the geometry of the space in a similar way as the deformation method. If E is the Euclidean space \mathbb{R}^2 , the simple SPDE

$$(1 - \Delta_E)u(\mathbf{s}) = \sqrt{4\pi}\mathcal{W}_E(\mathbf{s}), \quad \mathbf{s} \in E, \quad (8)$$

generates a stationary Matérn GRF with range $\rho = \sqrt{8}$, marginal variance $\sigma^2 = 1$, and smoothness $\nu = 1$. We introduce spatially varying distances in the space by giving the space geometric structure according to the metric tensor $\mathbf{g}(\mathbf{s}) = R(\mathbf{s})^{-2}\mathbf{I}_2$, where $R(\cdot)$ is a strictly positive scalar function. This locally scales distances by a factor $R(\mathbf{s})^{-1}$,

$$d\sigma^2 = [ds_1 \quad ds_2] \mathbf{g}(\mathbf{s}) \begin{bmatrix} ds_1 \\ ds_2 \end{bmatrix} = R(\mathbf{s})^{-2}(ds_1^2 + ds_2^2), \quad (9)$$

where $d\sigma$ is the line element, and s_1 and s_2 are the two coordinates of $E = \mathbb{R}^2$.

The non-stationarity in the correlation structure is then described through the spatially varying geometry in Equation (9), which results in a curved two-dimensional manifold that must be embedded in a space with dimension higher than 2 to exist in Euclidean space. The resulting spatial field does not have exactly constant marginal variance because the curvature of the space is non-constant unless $R(\cdot)$ does not vary in space, but there will be less interaction between $R(\cdot)$ and the marginal variance than between $\kappa(\cdot)$ and the marginal variance. And when $R(\cdot)$ varies slowly, the variation in marginal variances is small.

We can relate the Laplace-Beltrami operator in E to the usual Laplacian in \mathbb{R}^2 through

$$\Delta_E = \frac{1}{\sqrt{\det(g)}} \nabla_{\mathbb{R}^2} \cdot (\sqrt{\det(g)} g^{-1} \nabla_{\mathbb{R}^2}) = R(\mathbf{s})^2 \Delta_{\mathbb{R}^2},$$

and the Gaussian standard white noise in E to the Gaussian standard white noise in \mathbb{R}^2 through

$$\mathcal{W}_E(\mathbf{s}) = \det(g)^{1/4} \mathcal{W}_{\mathbb{R}^2}(\mathbf{s}) = R(\mathbf{s})^{-1} \mathcal{W}_{\mathbb{R}^2}(\mathbf{s}).$$

Thus the equivalent SPDE in \mathbb{R}^2 can be written as

$$R(\mathbf{s})^{-2} [1 - R(\mathbf{s})^2 \Delta_{\mathbb{R}^2}] u(\mathbf{s}) = R(\mathbf{s})^{-1} \sqrt{4\pi} \mathcal{W}_{\mathbb{R}^2}(\mathbf{s}), \quad \mathbf{s} \in \mathbb{R}^2,$$

where the first factor is needed because the volume element $dV_E = \sqrt{\det(g)} dV_{\mathbb{R}^2}$. The SPDE can be written as

$$(R(\mathbf{s})^{-2} - \Delta_{\mathbb{R}^2}) u(\mathbf{s}) = \sqrt{4\pi} R(\mathbf{s})^{-1} \mathcal{W}_{\mathbb{R}^2}, \quad \mathbf{s} \in \mathbb{R}^2, \quad (10)$$

in Euclidean space, but we can interpret the non-stationarity through the implied metric tensor. The procedure is similar to the simple reparametrization $\kappa(\cdot) = R(\cdot)^{-1}$, but the extra factor on the right-hand side of the equation reduces the variability of the marginal variances due to changes in $\kappa(\cdot)$.

For example, the space $[0, 9] \times [0, 3]$ with the Euclidean distance metric can be visualized as a rectangle, which exists in \mathbb{R}^2 , or as a half cylinder with radius $3/\pi$ and height 9, which exists in \mathbb{R}^3 , but if the space is given the spatially varying metric tensor defined by the local range function

$$R(s_1, s_2) = \begin{cases} 1 & 0 \leq s_1 < 3, 0 \leq s_2 \leq \pi, \\ (s_1 - 2) & 3 \leq s_1 < 6, 0 \leq s_2 \leq \pi, \\ 4 & 6 \leq s_1 \leq 9, 0 \leq s_2 \leq \pi, \end{cases} \quad (11)$$

the space cannot be embedded in \mathbb{R}^2 . With this metric tensor, the space is no longer flat, and must be embedded in \mathbb{R}^3 as, for example, the deformed cylinder shown in Figure 6. Thus, solving Equation (10) with the spatially varying coefficient is the same as solving Equation (8) on the deformed space. This means that unlike the deformation method, a spatially varying $R(\cdot)$ does not correspond to a deformation of \mathbb{R}^2 to \mathbb{R}^2 , but rather from \mathbb{R}^2 to a higher-dimensional space.

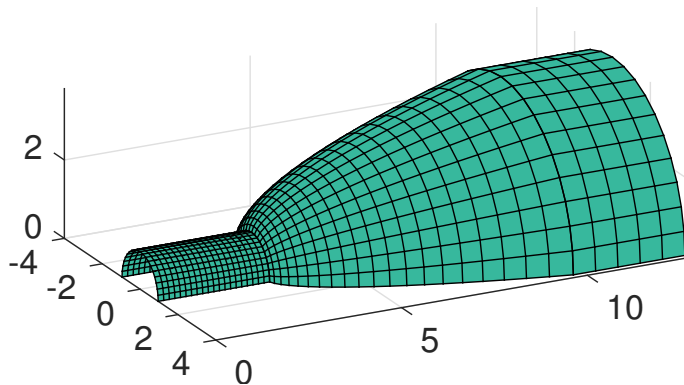


Figure 6: Half cylinder deformed according to the spatially varying metric tensor. The lines formed a regular grid on the half cylinder before deformation.

Since the variation in the marginal variances due to variations in the local ranges is small if $R(\cdot)$ does not vary too much, we introduce a separate function $S(\cdot)$ that controls the marginal standard deviations of the process and limit the SPDE to a region of interest, \mathcal{D} , with Neumann boundary conditions,

$$(R(s)^{-2} - \Delta_{\mathbb{R}^2}) \left(\frac{u(\mathbf{s})}{S(\mathbf{s})} \right) = \sqrt{4\pi} R(s)^{-1} \mathcal{W}_{\mathbb{R}^2}(\mathbf{s}), \quad \mathbf{s} \in \mathcal{D}.$$

This introduces boundary effects as was discussed in the paper by Lindgren et al. (2011), but we will not discuss the effects of the boundary in this paper.

This SPDE allows for greater separation of the parameters that affect correlation structure and the parameters that affect marginal standard deviations than the previous approach, and demonstrates the usefulness of careful consideration of how the spatially varying behaviour is introduced and parametrized. The SPDE derived based on the metric tensor allows for separate priors for correlation structure and marginal standard deviations through expansions of $\log(R(\cdot))$ and $\log(S(\cdot))$ into bases.

6.2 Setting priors on the parameters

There are two sources of non-stationarity in the flexible extension from stationarity: a function $R(\cdot)$ that controls local range and a function $S(\cdot)$ that controls the marginal standard deviation. The degree of flexibility in each of these sources of non-stationarity must be controlled to limit the risk of overfitting. Due to the issues of infinite KLDs discussed in Section 2.1, we will not follow the PC prior framework, but instead use a construction motivated by the principles of the PC priors to make the non-stationary model contract towards a base model of stationarity. Denote by $\boldsymbol{\theta}$ the extra parameters added to the GRF that move the model away from the base model of stationarity, $\boldsymbol{\theta} = \mathbf{0}$. The prior on $\boldsymbol{\theta}$ will be constructed conditionally on the parameters of the stationary GRF, ρ and σ^2 , and for each choice of these parameters, $\boldsymbol{\theta}$ should shrink towards $\mathbf{0}$.

We parametrize the local distance, $R(\cdot)$, and the approximate marginal standard deviations, $S(\cdot)$, through

$$\begin{aligned}\log(R(\mathbf{s})) &= \log\left(\frac{\rho}{\sqrt{8}}\right) + \sum_{i=1}^{n_1} \theta_{1,i} f_{1,i}(\mathbf{s}), \quad \mathbf{s} \in \mathcal{D}, \\ \log(S(\mathbf{s})) &= \log(\sigma) + \sum_{i=1}^{n_2} \theta_{2,i} f_{2,i}(\mathbf{s}), \quad \mathbf{s} \in \mathcal{D},\end{aligned}\tag{12}$$

where $\{f_{1,i}\}$ is a set of basis functions for the local range centred such that $\langle f_{1,i}, 1 \rangle_{\mathcal{D}} = 0$, for $i = 1, 2, \dots, n_1$, and $\{f_{2,i}\}$ is a set of basis functions for the marginal standard deviations centred such that $\langle f_{2,i}, 1 \rangle_{\mathcal{D}} = 0$ for $i = 1, 2, \dots, n_2$. We collect the parameters in vectors $\boldsymbol{\theta}_1 = (\theta_{1,1}, \dots, \theta_{1,n_1})$ and $\boldsymbol{\theta}_2 = (\theta_{2,1}, \dots, \theta_{2,n_2})$ such that $\boldsymbol{\theta}_1$ controls the non-stationarity in the correlation structure and $\boldsymbol{\theta}_2$ controls the non-stationarity in the marginal standard deviations.

We want the prior for each source of non-stationarity to be invariant to scaling of the covariates and to handle linear dependences between the covariates in a reasonable way, and we follow the basic idea of the g-priors (Zellner, 1986) (with $g = 1$),

$$\boldsymbol{\theta}_1 | \tau_1 \sim \mathcal{N}(\mathbf{0}, \tau_1^{-1} \mathbf{S}_1^{-1}) \quad \text{and} \quad \boldsymbol{\theta}_2 | \tau_2 \sim \mathcal{N}(\mathbf{0}, \tau_2^{-1} \mathbf{S}_2^{-1}),$$

where S_1 is the Gramian,

$$S_{1,i,j} = \frac{\langle f_{1,i}, f_{1,j} \rangle_{\mathcal{D}}}{\langle 1, 1 \rangle_{\mathcal{D}}}, \quad \text{for } i, j = 1, 2, \dots, n_1,$$

and S_2 is the Gramian,

$$S_{2,i,j} = \frac{\langle f_{2,i}, f_{2,j} \rangle_{\mathcal{D}}}{\langle 1, 1 \rangle_{\mathcal{D}}}, \quad \text{for } i, j = 1, 2, \dots, n_2.$$

In this set-up the Gramians account for the structure in the basis functions and the strictness of the priors are controlled by two precision parameters τ_1 and τ_2 . If the precision parameters are fixed hyperparameters, the resulting priors are Gaussian. However, the Gaussian probability density is flat at zero due to the infinite differentiability of the density function, and we prefer a prior that has a spike at zero.

This can be achieved by selecting the hyperpriors to be the PC prior for the precision parameter in a Gaussian distribution (Simpson et al., 2015), which is designed to shrink towards a base model of no effect. We combine the selection for the hyperpriors with an *a priori* ansatz that the independence between the correlation structure and the marginal variance in the prior for the stationary model also can be applied to the non-stationarity,

$$\pi(\tau_1) = \frac{\lambda_1}{2} \tau_1^{-3/2} \exp\left(-\lambda_1 \tau_1^{-1/2}\right) \quad \text{and} \quad \pi(\tau_2) = \frac{\lambda_2}{2} \tau_2^{-3/2} \exp\left(-\lambda_2 \tau_2^{-1/2}\right).$$

These hyperpriors for the precision parameters have so heavy tails that integrating them out will introduce infinite spikes in the marginal priors for $\boldsymbol{\theta}_1$ and $\boldsymbol{\theta}_2$ at zero.

The hyperparameters λ_1 and λ_2 control the spread of the priors and can be selected either based on expert knowledge or on frequentist properties. The parameters $\boldsymbol{\theta}_1$ and $\boldsymbol{\theta}_2$ give multiplicative effects to local range and marginal standard deviations, respectively, and one possibility is to control the size of the multiplicative effect through

$$\begin{aligned} \text{Prob} \left(\max_{\mathbf{s} \in \mathcal{D}} \left| \log \left(\frac{R(\mathbf{s})}{\rho/\sqrt{8}} \right) \right| > C_1 \mid \rho, \sigma^2 \right) &= \text{Prob} \left(\max_{\mathbf{s} \in \mathcal{D}} \left| \log \left(\frac{R(\mathbf{s})}{\rho/\sqrt{8}} \right) \right| > C_1 \right) = \alpha_1, \\ \text{Prob} \left(\max_{\mathbf{s} \in \mathcal{D}} \left| \log \left(\frac{S(\mathbf{s})}{\sigma^2} \right) \right| > C_2 \mid \rho, \sigma^2 \right) &= \text{Prob} \left(\max_{\mathbf{s} \in \mathcal{D}} \left| \log \left(\frac{S(\mathbf{s})}{\sigma^2} \right) \right| > C_2 \right) = \alpha_2. \end{aligned}$$

One can see from Equation (12) that the relative differences do not depend on the parameters of the stationary model, and the full prior factors as $\pi(\rho, \sigma^2, \boldsymbol{\theta}) = \pi(\rho)\pi(\sigma^2)\pi(\boldsymbol{\theta}_1)\pi(\boldsymbol{\theta}_2)$.

In practice, it is difficult to have an informed, *a priori* opinion on the non-stationary part of the model, but the hyperparameters λ_1 and λ_2 can be chosen in such a way that they give a conservative prior. Since stationarity is our base model and the non-stationarity is provided as extra flexibility, we will require that the hyperparameters are set such that the inference behaves well when the true data-generating distribution is stationary. We propose to set the hyperparameter by first fitting the stationary model, using the maximum a posteriori estimate of the parameters to make multiple simulated datasets from the stationary GRF and nugget effect, fit the non-stationary GRF with a nugget effect to each dataset, and calculate the frequentist coverage of the non-stationarity parameters. The hyperparameters can then be set such that the coverage of the credible intervals of the non-stationary parameters is close to nominal coverage. This ensures that the prior provides enough regularization that each posterior marginal for the non-stationarity parameters do not suggest non-stationarity when a stationary data-generating function is used.

6.3 Example: Annual precipitation in southern Norway

We use a dataset consisting of total annual precipitation for the one year period September 1, 2008, to August 31, 2009, for the 233 measurement stations in southern Norway shown in Figure 7. The dataset was used by Ingebrigtsen et al. (2014, 2015) to study the use of covariates in the covariance structure and associated priors. They used an intercept and a linear effect of the elevations of the stations in the first-order structure and used the elevation as a covariate in the second-order structure. We will follow their choice of covariates in the first-order structure, but add the magnitude of the gradient of the elevation in addition to the elevation as a covariate in the second-order structure. The additional covariate is added to demonstrate that the proposed prior deals appropriately with multiple covariates and to see the effect of the additional covariate on the fit of the model.

We use a simple geostatistical model

$$y_i = \beta_0 + x_i\beta_1 + u(\mathbf{s}_i) + \epsilon_i, \quad i = 1, 2, \dots, 233, \quad (13)$$

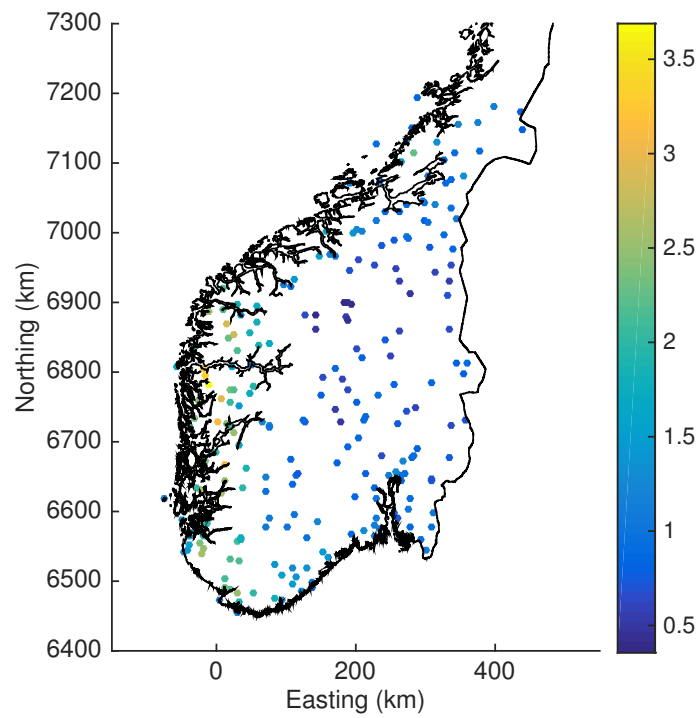


Figure 7: Total precipitation for the one year period September 1, 2008, to August 31, 2009, for 233 measurement stations in southern Norway measured in meters. Coordinate system is UTM33.

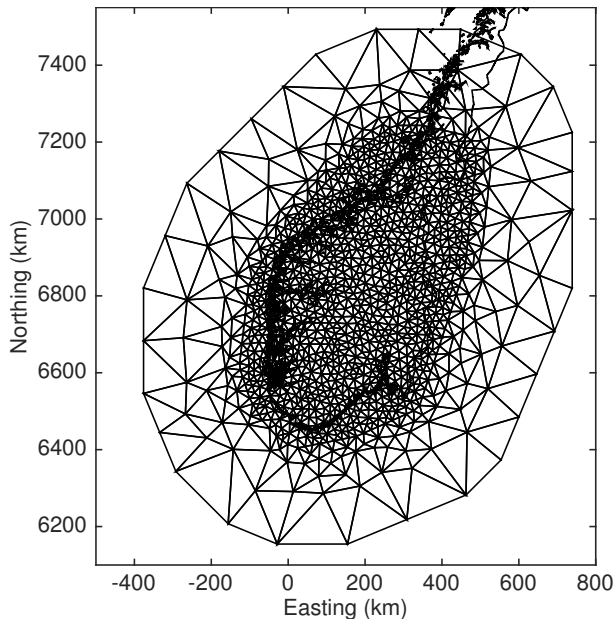


Figure 8: Mesh used for the SPDE approach.

where for station i , y_i is the observation made at location \mathbf{s}_i , x_i is the elevation of the station, (β_0, β_1) are the coefficients of the fixed effects, $u(\cdot)$ is the spatial effect, and ϵ_i is the nugget effect. The nuggets are i.i.d. $\epsilon_i \sim \mathcal{N}(0, \sigma_N^2)$, and the spatial effect is constructed with the SPDE approach (Lindgren et al., 2011) and the stationary version has two parameters: spatial range ρ and marginal variance of the spatial field σ^2 .

In the SPDE approach the spatial field is defined on a triangular mesh and the values of the spatial field within the triangles are defined through linear interpolation based on the values on the nodes of the mesh. This means that the elevation covariate in the first-order structure is only needed at each observation location, but that the elevation and gradient covariates in the second-order structure are needed at every location within the triangulation. We use the mesh shown in Figure 8 and project elevation and gradient values from the high resolution digital elevation map GLOBE (Hastings et al., 1999) onto the mesh. The projection is piece-wise linear on each triangle of the mesh and minimizes the integrated square deviation over the domain covered by the mesh. This results in the piece-wise linear covariates shown in Figure 9.

The stationary model is given priors that satisfy

$$P(\rho < 10) = 0.05, \quad P(\sigma_s > 3) = 0.05 \quad \text{and} \quad P(\sigma_n > 3) = 0.05,$$

and fitted to the data with INLA (Rue et al., 2009). With this prior we consider a standard deviation greater than 3 large for both the process and the nugget effect, and a range less than 10 km unlikely based on the spatial scale that we are working on. We are not interested in the stationary model beyond using the MAP estimates, $\hat{\sigma}_N = 0.13$, $\hat{\rho} = 219$ and $\hat{\sigma} = 0.72$, for setting the hyperparameters in the prior for the non-stationarity,

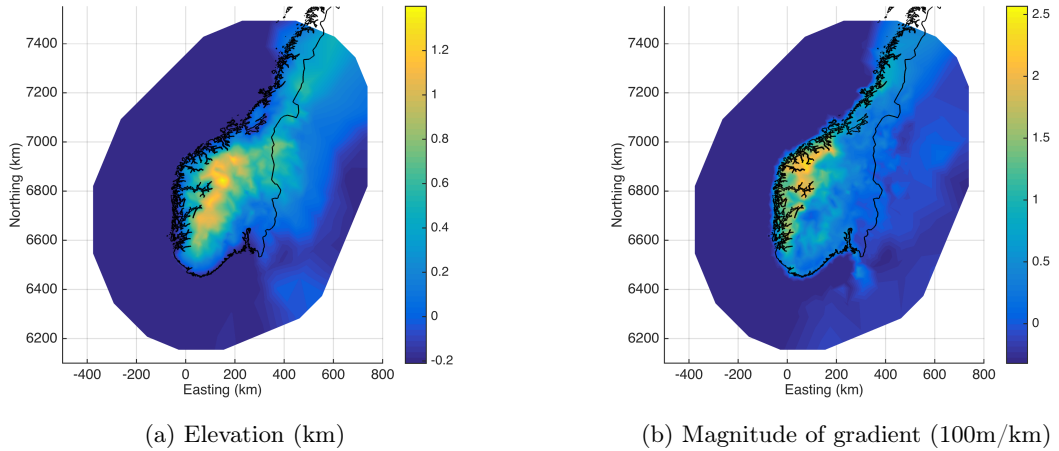


Figure 9: The covariates (a) elevation and (b) magnitude of the gradient used for the covariance structure.

and to compare the predictions scores with that of the non-stationary model.

The coefficients, $\boldsymbol{\theta}_1$, of the two linear covariates in $\log(R(\cdot))$ are given the prior

$$\begin{aligned}\boldsymbol{\theta}_1 | \tau_1 &\sim \mathcal{N}(\mathbf{0}, S_1 / \sqrt{\tau_1}) \\ \tau_1 &\sim \frac{\lambda_1}{2} \tau_1^{-3/2} e^{-\lambda_1 / \sqrt{\tau_1}}\end{aligned}$$

as described in the previous section, and the coefficients, $\boldsymbol{\theta}_2$, of the two linear covariates in $\log(S(\cdot))$ are given a similar prior, but with hyperparameter λ_2 . The non-stationary model is more difficult to fit in the INLA framework than the stationary model because the priors for $\boldsymbol{\theta}_1$ and $\boldsymbol{\theta}_2$ have infinite spikes in $\mathbf{0}$ that makes the posteriors non-Gaussian in the area around the origin. The optimization can be improved by reparametrizing as $\boldsymbol{\theta}'_1 = \boldsymbol{\theta}_1 \sqrt{\tau_1}$ and $\boldsymbol{\theta}'_2 = \boldsymbol{\theta}_2 \sqrt{\tau_2}$, but the marginal posteriors will not be sufficiently peaked at the origin and will miss the multimodality that should be present when there is a mode close to zero. However, we still use INLA as a fast approximation for the repeated fitting of the datasets needed for selecting the hyperparameters of the prior for non-stationarity.

Specifically, we use the MAP estimates of the stationary model to simulate 100 datasets from the stationary model with $\beta_0 = \beta_1 = 0$, set values for the hyperparameters λ_1 and λ_2 , fit a non-stationary model with $\beta_0 = \beta_1 = 0$ to each of datasets, and calculate the frequentist coverage of the the 95% credible intervals of the non-stationarity parameters. We tried several values for the hyperparameters λ_1 and λ_2 and found that $\lambda_1 = \lambda_2 = 20$ provides coverage that is close to the nominal 95%. These values are used for the hyperparameters when fitting the data to the full model in Equation (13) with a non-stationary spatial effect. The lack of some mass at zero for the posteriors calculated by INLA is likely to make the procedure overly conservative.

The non-stationary model was then fitted using an MCMC sampler and the resulting

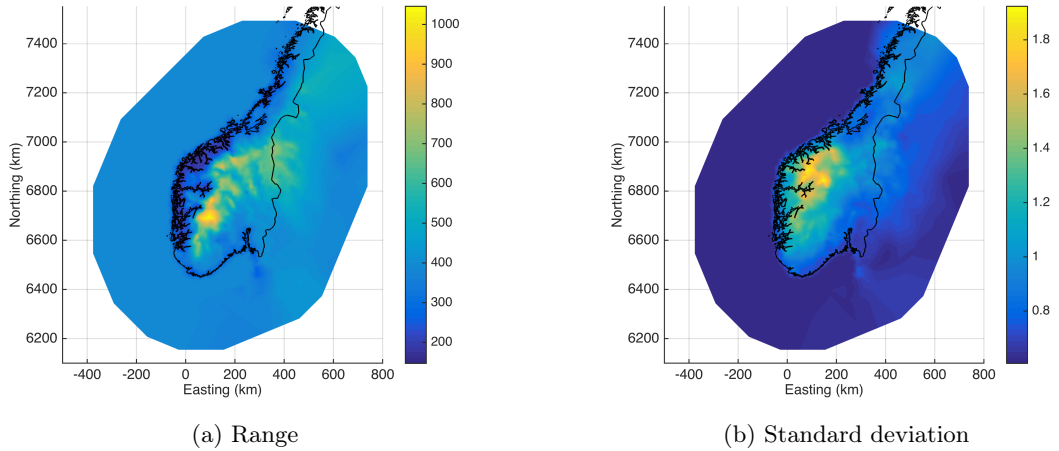


Figure 10: Posterior mean of (a) range and (b) standard deviation.

posterior means of the range and the standard deviation are shown in Figure 10. From Figure 11 one can see that the spatially varying range and standard deviation leads to non-stationarity in the correlation structure and the marginal standard deviations of the spatial effect. However, the effect in standard deviations appear to be stronger than the effect of the spatially varying range. The posteriors for the multiplicative effects on the stationary range and standard deviation for the western location in Figure 11a shown in Figure 12 shows that the effects are significant in that location. The posterior probabilities for the effects to be less than 1 and greater than 1 are 99% and 99%, respectively. This shows that the the more flexible non-stationary model is preferring to move away from the stationary model even under a conservatively selected prior.

A simple estimator of the the leave-one-out log-score can be made directly from the samples of the MCMC sampler, and we find the score 0.13 for the stationary model and 0.22 for the non-stationary model. The leave-one-out CRPS can be calculated based on a Gaussian approximation of the posterior by matching the mean and variance like done by Ingebrigtsen et al. (2014, 2015). This results in a CRPS of 0.111 for the stationary model and a CRPS of 0.101 for the non-stationary model. These values are lower than 0.1267 and 0.1241, respectively, that was found in Ingebrigtsen et al. (2014), but their values were based on 13-fold cross validation. The CRPS in the later paper Ingebrigtsen et al. (2015) are not directly comparable as they are based on fits of multiple years of data. The non-stationary GRF leads to better scores, and experimenting with the strictness of the prior showed that further improvements were possible by making the prior weaker, but that making the prior too weak leads to worse scores. The prior and the procedure for selecting the hyperparameters appears to introduce a reasonable level of conservativeness for this dataset. The estimates for CRPS without using the approximation for the predictive distributions are 0.092 for the stationary model and 0.083 for the non-stationary model, which means that a Gaussian approximation to the

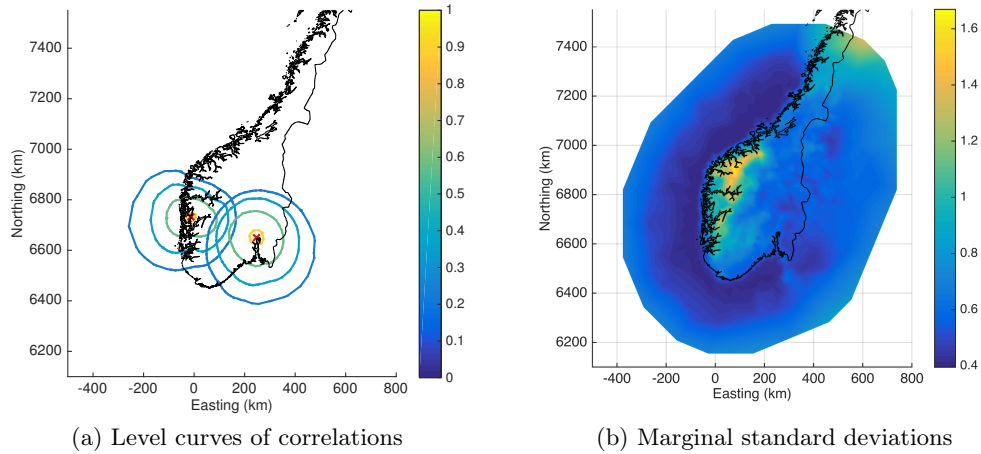


Figure 11: Covariance structure described through (a) 0.90, 0.57, 0.36 and 0.22 level curves of correlation with respect to the two locations marked with red crosses and (b) marginal standard deviations.

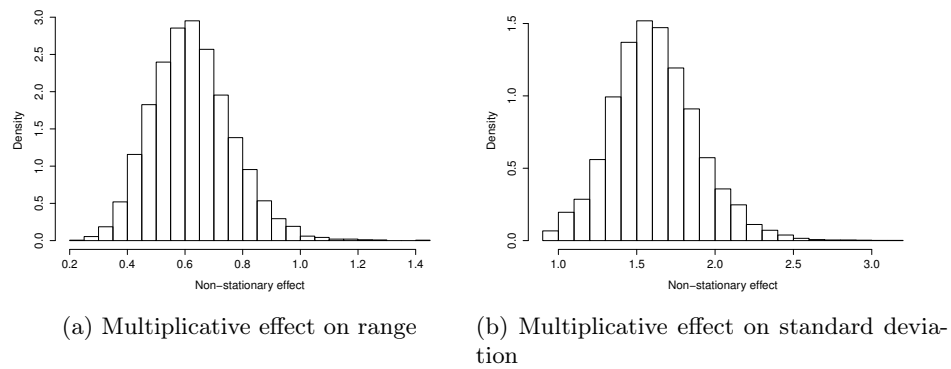


Figure 12: Posteriors of the multiplicative effect on the stationary (a) range and (b) standard deviation at the western location in Figure 11a.

predictive distribution is sub-optimal.

Figure 11 gives the impression that the non-stationarity in the correlation structure is weak and that the non-stationarity in the marginal standard deviations is clearer. If we run the model with the same hyperparameters and remove the non-stationarity in the local range, the CRPS is 0.086, and if we remove the non-stationarity in the marginal standard deviations, the CRPS is 0.081. This shows that the covariates in the local range are contributing more to the improved predictions than the covariates in the standard deviation, and that using all four covariates has degraded the performance slightly compared to using only a non-stationary local range. This demonstrates how difficult it is to ensure that adding covariates in the second-order structure always leads to better predictions. A conservative prior helps avoiding severe overfitting, but if prediction is the main goal, the prediction scores of the models should be compared.

7 Discussion

The guiding principle for constructing priors in this paper has been to limit flexibility. The stationary GRF is an extension of no spatial field and the prior should shrink towards no effect, and the non-stationary GRF is an extension of the stationary GRF and the prior should shrink towards stationarity. This idea of a base model and a flexible extension of that base model is one of the central points of the PC prior framework, and the prior on the range and the marginal variance was constructed directly within this framework, whereas the prior on the non-stationary extension was guided by the framework.

The main issue in each case is that there is not enough information about the parameters of the GRF under in-fill asymptotics. Even for the two-parameter stationary model the posteriors do not contract, and for more complex non-stationary GRFs one risks severe overfitting. The constructed priors provides the opportunity to limit the flexibility by introducing prior knowledge about the process and limiting the risk of overfitting. Additionally, the joint PC prior for the range and the marginal variance for the Matérn GRF is easy to implement and quick to compute, works with any observation process and can be used in hierarchical models, and does not depend of the sampling design of the process. Further, the stationary prior can be extended to a prior for a full non-stationary GRF that has covariates both in the correlation structure and in the marginal standard deviations.

Setting the hyperparameters for the stationary part of the model can be done based on statements about what constitutes a large standard deviation and what constitutes a small range. This allows the users to choose to limit the movement towards intrinsic models along the ridge in the likelihood and thus provide more sensible posterior inference for the problem at hand. We observe sensitivity when one misses by one order in the prior specification or set too high lower limits or too low upper limits, but in return the credible intervals are shorter than for the objective priors.

When setting the hyperparameters for the non-stationary GRF, it is difficult to elicit expert knowledge since the second-order structure is not observed directly, and we discuss an alternative way to set the hyperparameters based on the frequentist coverage of the

credible intervals. Using the new prior and the associated scheme for selecting the hyperparameters, we find a better fit for the non-stationary GRF than with the stationary GRF applied to the dataset of annual precipitation in southern Norway measured both in leave-one-out CRPS and log scores.

The paper shows that the PC priors provide a helpful tool for setting priors on parameters for which it up until now has been difficult to come up with theoretically founded priors. But also that the ideas of the framework are helpful for constructing priors that limit flexibility even when the exact derivation is not possible.

A Derivation of the Kullback-Leibler divergence for κ

We parametrize the Matérn GRF through $\kappa = \sqrt{8\nu}/\rho$ and

$$\tau = \frac{\Gamma(\nu)}{(4\pi)^{d/2}\Gamma(\nu + d/2)\sigma^2\kappa^{2\nu}},$$

where ρ is the range, σ^2 is the marginal variance, ν is the smoothness, and d is the dimension of the base space. If τ is fixed and the process is observed on a bounded observation window, the Kullback-Leibler Divergence (KLD) between the distributions described by $\kappa = \kappa_0 > 0$ and $\kappa = \kappa_1 > 0$ is finite and it is possible to use the KLD to quantify how different the distributions are. The KLD of the probability measure Q from the probability measure P is defined by

$$D_{\text{KL}}(P||Q) = \int_{\mathcal{X}} \log \left(\frac{dP}{dQ} \right) dP, \quad (14)$$

where dP/dQ is the Radon-Nikodym derivative of P with respect to Q , and expresses the information lost when Q is used to approximate P .

Fix τ and ν , and let u_κ denote the Matérn GRF with parameter κ . Lindgren et al. (2011) showed that this GRF is a solution of the stochastic partial differential equation (SPDE)

$$(\kappa^2 - \Delta)^{\alpha/2}(\sqrt{\tau}u_\kappa(\mathbf{s})) = \mathcal{W}(\mathbf{s}), \quad \mathbf{s} \in \mathbb{R}^d, \quad (15)$$

where $\alpha = \nu + d/2$ and \mathcal{W} is standard Gaussian white noise, and that the spectral density of u_κ is given by

$$f_\kappa(\mathbf{w}) = \left(\frac{1}{2\pi} \right)^d \frac{1}{\tau(\kappa^2 + \mathbf{w}^T \mathbf{w})^\alpha}. \quad (16)$$

We approximate the GRF u_κ with the solution \tilde{u}_κ of SPDE (15) restricted to the domain $\mathcal{D} = [-L/2, L/2]^d$ with periodic boundary conditions. The spectral density of \tilde{u}_κ is discrete and the spatial field can be written as

$$\tilde{u}_\kappa(\mathbf{s}) = \sum_{\mathbf{k} \in \mathbb{Z}^d} z_{\mathbf{k}} e^{i\langle 2\pi\mathbf{k}/L, \mathbf{s} \rangle},$$

where $\{z_{\mathbf{k}}\}$ are independent Gaussian random variables with variances given by

$$\begin{aligned} \lambda_{\mathbf{k}}(\kappa) &= \frac{1}{\tau(\kappa^2 + \|2\pi\mathbf{k}/L\|^2)^\alpha} \frac{\text{Var}[\langle \mathcal{W}, e^{i\langle 2\pi\mathbf{k}/L, \mathbf{s} \rangle} \rangle_{\mathcal{D}}]}{\langle e^{i\langle 2\pi\mathbf{k}/L, \mathbf{s} \rangle}, e^{i\langle 2\pi\mathbf{k}/L, \mathbf{s} \rangle} \rangle_{\mathcal{D}}^2} \\ &= \frac{1}{L^d} \frac{1}{\tau(\kappa^2 + \|2\pi\mathbf{k}/L\|^2)^\alpha}. \end{aligned} \quad (17)$$

The KLD between \tilde{u}_κ and \tilde{u}_{κ_0} (based on Bogachev (1998, Thm. 6.4.6)),

$$\begin{aligned} 2\text{KLD}(\kappa||\kappa_0) &= \sum_{\mathbf{k} \in \mathbb{Z}^d} \left[\frac{\lambda_{\mathbf{k}}(\kappa_0)}{\lambda_{\mathbf{k}}(\kappa)} - 1 - \log \frac{\lambda_{\mathbf{k}}(\kappa_0)}{\lambda_{\mathbf{k}}(\kappa)} \right] \\ &= \sum_{\mathbf{k} \in \mathbb{Z}^d} \left[\frac{(\kappa_0^2 + \|2\pi\mathbf{k}/L\|^2)^\alpha}{(\kappa^2 + \|2\pi\mathbf{k}/L\|^2)^\alpha} - 1 - \log \frac{(\kappa_0^2 + \|2\pi\mathbf{k}/L\|^2)^\alpha}{(\kappa^2 + \|2\pi\mathbf{k}/L\|^2)^\alpha} \right] \end{aligned} \quad (18)$$

is a simple expression involving only the spectral densities of the processes. The sum can be turned into a Riemann sum by scaling it with the step-size to the power of d ,

$$\begin{aligned} & 2 \left(\frac{2\pi}{L} \right)^d \text{KLD}(\kappa || \kappa_0) \\ &= \sum_{\mathbf{k} \in \mathbb{Z}^d} \left(\frac{2\pi}{L} \right)^d \left[\frac{(\kappa_0^2 + \|2\pi\mathbf{k}/L\|^2)^\alpha}{(\kappa^2 + \|2\pi\mathbf{k}/L\|^2)^\alpha} - 1 - \log \frac{(\kappa_0^2 + \|2\pi\mathbf{k}/L\|^2)^\alpha}{(\kappa^2 + \|2\pi\mathbf{k}/L\|^2)^\alpha} \right] \\ &= \int_{\mathbb{R}^d} \left[\frac{f_\kappa(\mathbf{w})}{f_{\kappa_0}(\mathbf{w})} - 1 - \log \frac{f_\kappa(\mathbf{w})}{f_{\kappa_0}(\mathbf{w})} \right] d\mathbf{w} + E(L, \kappa_0), \end{aligned}$$

where $E(L, \kappa_0)$ is the error in the Riemann sum.

We are interested in the case $\kappa_0 = 0$, and the Riemann sum will only converge if the limits $\kappa_0 \rightarrow 0$ and $L \rightarrow \infty$ are taken in such a way that the zero-frequency term converges. The zero-frequency term

$$\left(\frac{2\pi}{L} \right)^d \left[\left(\frac{\kappa_0^2}{\kappa^2} \right)^\alpha - 1 - \alpha \log \frac{\kappa_0^2}{\kappa^2} \right],$$

converges to zero if L tends to infinity in such a way that $L = o(\kappa_0^{-1})$, and we apply this relationship between L and κ_0 and introduce the scaled KLD

$$\text{K}\tilde{\text{L}}\text{D}(\kappa || 0) = \lim_{\kappa_0 \rightarrow 0} \left(\frac{2\pi}{L} \right)^d \text{KLD}(\kappa || \kappa_0) = \frac{1}{2} \int_{\mathbb{R}^d} \left[\frac{(\mathbf{w}^\text{T} \mathbf{w})^\alpha}{(\kappa^2 + \mathbf{w}^\text{T} \mathbf{w})^\alpha} - 1 - \log \frac{(\mathbf{w}^\text{T} \mathbf{w})^\alpha}{(\kappa^2 + \mathbf{w}^\text{T} \mathbf{w})^\alpha} \right] d\mathbf{w}.$$

We perform the change variables $\mathbf{w} = \kappa \mathbf{y}$ and find that

$$\text{K}\tilde{\text{L}}\text{D}(\kappa || 0) = \frac{1}{2} \int_{\mathbb{R}^d} \left[\frac{(\mathbf{y}^\text{T} \mathbf{y})^\alpha}{(1 + \mathbf{y}^\text{T} \mathbf{y})^\alpha} - 1 - \log \frac{(\mathbf{y}^\text{T} \mathbf{y})^\alpha}{(1 + \mathbf{y}^\text{T} \mathbf{y})^\alpha} \right] \kappa^d d\mathbf{y} = \kappa^d \text{K}\tilde{\text{L}}\text{D}(1 || 0) \propto \kappa^d \quad (19)$$

if $\text{K}\tilde{\text{L}}\text{D}(1 || 0)$ exists.

$\text{K}\tilde{\text{L}}\text{D}(1 || 0)$ can be expressed as an integral in n -dimensional spherical coordinates,

$$\text{K}\tilde{\text{L}}\text{D}(1 || 0) = C_d \int_0^\infty \left[\left(\frac{r^2}{1+r^2} \right)^\alpha - 1 - \log \left(\frac{r^2}{1+r^2} \right)^\alpha \right] r^{d-1} dr, \quad (20)$$

where C_d is a constant that varies with dimension. There are two issues: the behaviour for small r and the behaviour for large r . For $d = 1$,

$$\text{K}\tilde{\text{L}}\text{D}(1 || 0) \leq -C_1 \alpha \int_0^\infty \log \frac{r^2}{1+r^2} dr = \pi \alpha C_1,$$

and we can conclude that the behaviour around 0 is not a problem for any $d \geq 1$. The behaviour for large r can be studied through an expansion in $(1+r^2)^{-1}$. The part between the square brackets in Equation (20) behaves as

$$\frac{\alpha^2}{2} \frac{1}{(1+r^2)^2} + \mathcal{O} \left(\frac{1}{(1+r^2)^3} \right).$$

This means that we can find an $0 < r_0 < \infty$ such that

$$\begin{aligned} \int_0^\infty \left[\left(\frac{r^2}{1+r^2} \right)^\alpha - 1 - \log \left(\frac{r^2}{1+r^2} \right)^\alpha \right] r^{d-1} dr \\ \leq \text{Const} + \int_{r_0}^\infty \left[\frac{\alpha^2}{2} \frac{1}{(1+r^2)^2} + \frac{C}{(1+r^2)^3} \right] dr, \end{aligned}$$

where $C \geq 0$ is a constant. For $d \leq 3$ both terms on the right hand side are finite and based on this and the boundedness for $d = 1$, we can conclude that $\text{KLD}(1||0)$ is finite for $d \leq 3$.

B Tables for frequentist coverage study

The simulation study in Section 3 was run with four different priors: the PC prior (PriorPC), the Jeffreys' rule prior (PriorJe), a uniform prior on range on a bounded interval combined with the Jeffreys' prior for variance (PriorUn1) and a uniform prior on the log-range on a bounded interval combined with the Jeffreys' prior for variance (PriorUn2). For each prior a selection of hyperparameters were tested on datasets generated from true ranges $\rho_0 = 0.1$ and $\rho_0 = 1.0$, and the frequentist coverages of the 95% credible intervals and the lengths of the credible intervals were estimated. For $\rho_0 = 0.1$, PriorJe gave 97.0% coverage with average length 0.86 for range and 96.0% coverage with average length 2.7 for marginal variance, and for $\rho_0 = 1.0$, PriorJe gave 95.4% coverage with average length 445 for range and 94.4% coverage with average length of 355 for marginal variance. The results for PriorPC is given in Section 3 and the the results for the two other priors are collected in the tables:

Prior	$\rho_0 = 0.1$	$\rho_0 = 1.0$
PriorUn1	Table 5	Table 7
PriorUn2	Table 6	Table 8

References

- Berger, J. O., De Oliveira, V., and Sansó, B. (2001). Objective Bayesian analysis of spatially correlated data. *Journal of the American Statistical Association*, 96(456):1361–1374.
- Bogachev, V. I. (1998). *Gaussian measures*. Number 62. American Mathematical Soc.
- Hastings, D. A., Dunbar, P. K., Elphinstone, G. M., Bootz, M., Murakami, H., Maruyama, H., Masaharu, H., Holland, P., Payne, J., Bryant, N. A., Logan, T. L., Muller, J.-P., Schreier, G., and MacDonald, J. S. (1999). The global land one-kilometer base elevation (globe) digital elevation model, version 1.0.
- Ingebrigtsen, R., Lindgren, F., and Steinland, I. (2014). Spatial models with explanatory variables in the dependence structure. *Spatial Statistics*, 8:20–38.

Table 5: Frequentist coverage of 95% credible intervals for range and marginal variance when the true range $\rho_0 = 0.1$ using PriorUn1, where the average lengths of the credible intervals are shown in brackets.

(a) Range			
$A \setminus B$	2	20	200
$5 \cdot 10^{-2}$	0.901 [0.95]	0.901 [8.6]	0.847 [122]
$5 \cdot 10^{-3}$	0.935 [0.92]	0.918 [7.7]	0.887 [110]
$5 \cdot 10^{-4}$	0.948 [0.93]	0.929 [7.9]	0.893 [110]

(b) Marginal variance			
$A \setminus B$	2	20	200
$5 \cdot 10^{-2}$	0.952 [3.5]	0.941 [29]	0.895 [460]
$5 \cdot 10^{-3}$	0.945 [3.3]	0.937 [27]	0.907 [410]
$5 \cdot 10^{-4}$	0.953 [3.3]	0.925 [27]	0.921 [412]

Table 6: Frequentist coverage of 95% credible intervals for range and marginal variance when the true range $\rho_0 = 0.1$ using PriorUn2, where the average lengths of the credible intervals are shown in brackets.

(a) Range			
$A \setminus B$	2	20	200
$5 \cdot 10^{-2}$	0.986 [0.47]	0.979 [0.84]	0.988 [1.1]
$5 \cdot 10^{-3}$	0.976 [0.44]	0.950 [0.81]	0.966 [1.0]
$5 \cdot 10^{-4}$	0.932 [0.40]	0.945 [0.70]	0.944 [1.3]

(b) Marginal variance			
$A \setminus B$	2	20	200
$5 \cdot 10^{-2}$	0.949 [2.0]	0.962 [2.9]	0.965 [3.6]
$5 \cdot 10^{-3}$	0.968 [1.8]	0.960 [2.6]	0.959 [3.2]
$5 \cdot 10^{-4}$	0.948 [1.7]	0.960 [2.4]	0.949 [3.7]

Table 7: Frequentist coverage of 95% credible intervals for range and marginal variance when the true range $\rho_0 = 1$ using PriorUn1, where the average lengths of the credible intervals are shown in brackets.

(a) Range			
$A \setminus B$	2	20	200
$5 \cdot 10^{-2}$	0.995 [1.5]	0.831 [18]	0.593 [188]
$5 \cdot 10^{-3}$	0.996 [1.5]	0.818 [18]	0.539 [188]
$5 \cdot 10^{-4}$	0.994 [1.5]	0.844 [18]	0.537 [188]

(b) Marginal variance			
$A \setminus B$	2	20	200
$5 \cdot 10^{-2}$	0.979 [2.0]	0.857 [20]	0.614 [208]
$5 \cdot 10^{-3}$	0.979 [2.0]	0.821 [20]	0.585 [205]
$5 \cdot 10^{-4}$	0.969 [2.0]	0.828 [20]	0.561 [206]

Table 8: Frequentist coverage of 95% credible intervals for range and marginal variance when the true range $\rho_0 = 1$ using PriorUn2, where the average lengths of the credible intervals are shown in brackets.

(a) Range			
$A \setminus B$	2	20	200
$5 \cdot 10^{-2}$	0.980 [1.5]	0.959 [12]	0.933 [69]
$5 \cdot 10^{-3}$	0.974 [1.5]	0.954 [12]	0.954 [67]
$5 \cdot 10^{-4}$	0.964 [1.5]	0.953 [13]	0.956 [68]

(b) Marginal variance			
$A \setminus B$	2	20	200
$5 \cdot 10^{-2}$	0.955 [1.8]	0.952 [12]	0.945 [61]
$5 \cdot 10^{-3}$	0.962 [1.8]	0.943 [12]	0.941 [60]
$5 \cdot 10^{-4}$	0.939 [1.8]	0.946 [12]	0.953 [60]

- Ingebrigtsen, R., Lindgren, F., Steinsland, I., and Martino, S. (2015). Estimation of a non-stationary model for annual precipitation in southern Norway using replicates of the spatial field. *Spatial Statistics*, 14, Part C:338–364.
- Kazianka, H. (2013). Objective Bayesian analysis of geometrically anisotropic spatial data. *Journal of Agricultural, Biological, and Environmental Statistics*, 18(4):514–537.
- Kazianka, H. and Pilz, J. (2012). Objective Bayesian analysis of spatial data with uncertain nugget and range parameters. *Canadian Journal of Statistics*, 40(2):304–327.
- Lindgren, F., Rue, H., and Lindström, J. (2011). An explicit link between Gaussian fields and Gaussian Markov random fields: the stochastic partial differential equation approach. *Journal of the Royal Statistical Society: Series B (Statistical Methodology)*, 73(4):423–498.
- Oliveira, V. d. (2007). Objective Bayesian analysis of spatial data with measurement error. *The Canadian Journal of Statistics / La Revue Canadienne de Statistique*, 35(2):pp. 283–301.
- Paulo, R. (2005). Default priors for Gaussian processes. *The Annals of Statistics*, 33(2):556–582.
- Rue, H., Martino, S., and Chopin, N. (2009). Approximate Bayesian inference for latent Gaussian models by using integrated nested Laplace approximations. *Journal of the royal statistical society: Series b (statistical methodology)*, 71(2):319–392.
- Simpson, D., Rue, H., Martins, T., Riebler, A., and Sørbye, S. (2015). Penalising model component complexity: A principled, practical approach to constructing priors. *arXiv preprint arXiv:1403.4630*.
- Stein, M. L. (1999). *Interpolation of spatial data: some theory for kriging*. Springer.
- van der Vaart, A. W. and van Zanten, J. H. (2009). Adaptive Bayesian estimation using a Gaussian random field with inverse Gamma bandwidth. *Ann. Statist.*, 37(5B):2655–2675.
- Warnes, J. and Ripley, B. (1987). Problems with likelihood estimation of covariance functions of spatial gaussian processes. *Biometrika*, 74(3):640–642.
- Ying, Z. (1991). Asymptotic properties of a maximum likelihood estimator with data from a Gaussian process. *Journal of Multivariate Analysis*, 36(2):280 – 296.
- Zellner, A. (1986). On assessing prior distributions and Bayesian regression analysis with g-prior distributions. *Bayesian inference and decision techniques: Essays in Honor of Bruno De Finetti*, 6:233–243.
- Zhang, H. (2004). Inconsistent estimation and asymptotically equal interpolations in model-based geostatistics. *Journal of the American Statistical Association*, 99(465):250–261.